Analytical modeling of glass composite and metal reinforcement adhesion with cement-sand concrete

Victor Yartsev[1,*], *Botir* Giyasov[2], *Alexey* Nikolyukin[1], *Abdul Barei* Danish[1], *Timur* Giyasov[2], and *Dhafer* Aljaboobi[1]

[1]Tambov State Technical University, 106, Sovetskaya st., Tambov, 392000, Russia
[2]Moscow State University of Civil Engineering, Yaroslavskoe shosse, 26, Moscow, 129337, Russia

Abstract. Adhesion refers to the ability of concrete to resist slipping of reinforcement under loading in reinforced concrete products. The term "reinforced concrete" is considered as a uniform composite material as long as there is adhesion on the contact surface between the reinforcement and the concrete. In case of disruption of the reinforcement and concrete interaction, the construction is represented by separate elements. The aim of this work is to simulate the process of glass composite and metal reinforcement adhesion with cement concrete. To solve this problem, analytical modeling was performed in the ANSYS 19.0 Workbench software package, with the help of which the nature of damage accumulation in the rebar and the distribution of stresses in the concrete mass are determined.

1 Introduction

The problem of the reinforcement compliance and its mutual work with concrete under longitudinal load is one of the main problems of the reinforced concrete theory. Therefore, a huge number of domestic and foreign scientists took up this problem. The main theory describing the adhesion between a mutually displaced rebar and concrete is the theory by MM. Kholmyansky [1].

The objective of the current study is analysis of the stress-strain state (SSS) and determination of adhesion forces in the zone of interaction of reinforcement with concrete under the action of static axial pulling force.

To simplify the computational apparatus without reducing the overall accuracy in the adhesion analysis in the considered admissible displacement boundaries at the crack joint, an elastoplastic concrete deformation diagram (Prandtl diagram), on the basis of which M.M. Kholmyansky and his students (Fig. 1a) approximated the normal adhesion law, is used:

$$\tau_x = F(\mathrm{g_x}) = B\frac{ln(1+\alpha g)}{1+\alpha g} \quad (1)$$

* Corresponding author: kzis@nnn.tstu.ru

where B and α are adhesion parameters; g_x is the mutual displacement relative to the concrete mass.

Under the elastoplastic law, adhesion is characterized by the parameters τ_0 and g^*.

However, Fig. 1b shows the formation of the section with plastic deformations at exceeding the maximum stress value. Therefore, to establish the parameters τ_0 и g_0, the stress-strain state (SSS) in the area of anchoring the rebar in concrete should be considered for reinforced concrete structures [3].

To simplify this task, we consider a concrete prism centrally reinforced with a rebar with a symmetrically applied load from two sides (Fig. 1c).

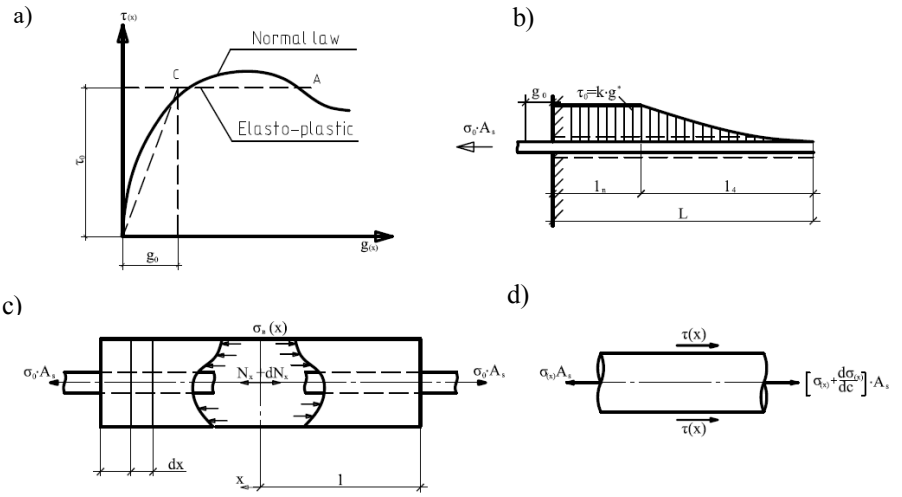

Fig. 1. Rebar and concrete interaction: **a)** «τ – g» diagram: elastoplastic and normal adhesion law [2]; **b)** distribution of adhesion stresses along the length of the reinforcement under elastoplastic law; **c)** calculation of the adhesion at the equilibrium of the concrete element; **d)** equilibrium of dx rebar element.

Consequently, the equilibrium equation for this problem takes the following form [1]:

$$\sigma_{\sigma(x)} = \mu(\sigma_0 - \sigma_s(x)) \tag{2}$$

The equation of the mutual deformation of the concrete and the rebar:

$$g(x) = g_0 \int_0^x [(\frac{\sigma_s(x)}{E_s} - \frac{\sigma_b(x)}{E_b})]\ dx \tag{3}$$

Using the previously obtained equation for shear stress τ (x), it takes the following form:

$$\tau(x,g) = \frac{E_s D}{4(l+n\mu)} \cdot \frac{d^2 g}{d\,x^2} \tag{4}$$

To form a system of equations physically describing τ_{ad} and g(x), the adhesion law is represented in the following form:

$$\tau(x,g) = F(g(x)) \tag{5}$$

The function F(g(x)) represents the adhesion law, in which the shear stresses τ (x) are taken as a constant value along the entire length of the rebar anchoring. The dependence F(g (x)) is proposed in the form of an elastoplastic diagram τ – g [4]:

$$F(g) = \begin{cases} kg(x), \text{при } g(x)/g^* \le 1 \\ kg^*, \text{при } g(x)/g^* \ge 1 \end{cases} \quad (6)$$

Having obtained the system of equations, the calculation at the elastic stage and later in the elastoplastic stage of work should be considered.

If the elastic stage is $g(x)/g^* \le 1$, with x = L, then the maximum displacement under loading is:

$$g_0 = \frac{\sigma_{s_0}(x)}{Ea\lambda} th\lambda L \quad (7)$$

The transition from the elastic stage to the elastoplastic one is characterized by the formation of sections with constant shear stresses τ_0 when the maximum displacement is reached $g_0 > g^*$.

If the elastoplastic stage is $g(x)/g^* \ge 1$, with x = L, then the maximum displacement under loading is:

$$g^* = \frac{\sigma_0}{\lambda L cth\lambda E_s} \quad (8)$$

The proposed system of equations allows to set the amount of the rebar displacement relatively to concrete. However, this dependence is applicable only for steel and composite reinforcement. In addition, it does not take into account elastoplastic deformations in concrete, which requires a deeper and more complete study of this problem.

2 Mathematical modeling for describing the rebar adhesion with concrete

This paper presents the results of the development of a mathematical model which takes into account the contact interaction of reinforcement with concrete [5].

The model of Menetrey-Willam [6] based on the Willam-Warnke yield surface [9], including the dependence on three independent invariants of the stress tensor, was adopted as a concrete model.

The Willam-Warnke yield surface differs from the Mohr–Coulomb yield surface by the absence of sharp edges, which may cause difficulties in solving the Mohr–Coulomb surface stress. It also has some characteristics of the Drucker-Prager model [8] and can simulate similar materials.

The Menetrey-Willam model is best suited for modeling the behavior of bound inert materials, since it allows to take into account the redistribution of the strength characteristics inside the material.

The Willam-Warnke yield surface in the Haigh-Westergaard stress coordinates is determined by the formula [7]:

$$f_{MW} = \frac{c_2}{c_3}\left[\sqrt{2}\xi + rp\right] + p^2 - \frac{1}{c_3} \quad (10)$$

where c_2 and c_3 are functions of material parameters and hardening/softening parameters, respectively.

The hardening and softening parameter is defined as follows [7]:

$$\overline{R_t} = R_t \Omega_{tc} \quad (11)$$

$$\overline{R_c} = R_c \Omega_c \quad (12)$$

$$\overline{R_b} = R_b \Omega_c \tag{13}$$

$$\Omega_{tc} = \begin{cases} \Omega_t, k_c \le k_{cm} \\ \Omega_c \Omega_t, k_c > k_{cm} \end{cases} \tag{14}$$

where k_{cm} is a material parameter; Ω_c and Ω_t are compression and hardening/softening functions, respectively, which depend on compression or hardening/softening parameters of k_c и k_t; R_t is the strength limit under uniaxial tension; R_c is the strength limit under uniaxial compression; R_b is the strength limit under biaxial compression.

To describe the work of the reinforcement material, a model of the generalized Hooke's law was adopted with the following assumptions:

- The material is considered to possess orthotropic properties when specifying physico-mechanical characteristics of the glass composite reinforcement (GCR). For this purpose the Orthotropic Elasticity material model [5] is used to describe the GCR operation. This model is also based on Hooke's law, but it has a material stiffness matrix in which the deformation characteristics in the YX and YZ planes are symmetric.
- As it was previously established, the primary reason of adhesion failure of GCR with concrete is the detachment of the reinforcement profile from the main rebar. A cohesive zone model (CZM) [9] is used to simulate this process, where the destruction of the binder matrix is regarded as a gradual separation of the reinforcement periodic profile surface from the main rebar with the subsequent delamination. In this model, the destruction of the contact surface occurs gradually, taking into account the accumulation of defects in the adhesive matrix inside the contact layer. The CZM is also used to simulate a bonding cement gel in the contact layer between the reinforcement and the concrete mass.

The CZM model is described by the following equation [9]:

$$\sigma_n = K_n u_n (1 - d_n) \tag{15}$$

where σ_n is stress; K_n is contact stiffness; u_n is tangential displacement in the contact area; d_n is a violation parameter of the adhesive matrix.

The violation parameter of the adhesive matrix:

$$d_n = \left(\frac{u_n - \overline{u_n}}{u_n}\right)\left(\frac{u_n^c}{u_n^c - \overline{u_n}}\right) \tag{16}$$

where $\overline{u_n}$ is displacement (slip length) in the contact area at the maximum stress; u_n^c is displacement in the contact area with the destruction of the adhesive matrix. At $\Delta_n \le 1$, at $\Delta_n > 1, 0 < d_n \le 1$, where $\Delta_n = \frac{u_n}{\overline{u_n}}$.

In this case, the critical destruction energy is calculated as:

$$G_{cn} = \frac{1}{2}\sigma_{max} u_n^c \tag{17}$$

- The GCR strength can be evaluated by various criteria, which can directly identify the probable pattern or mechanism of destruction, for example, indicate whether matrix or fiber failure will occur. Therefore, each strength criterion can be assigned a coefficient, which will show the priority in the analysis of the material destruction. For example, when stretching the GCR, the rebar external fibers are more likely to be destructed, and this criterion should be assigned a higher fiber destruction strength coefficient. In this paper, the strength criterion for the GCR is the Puck criterion [10], which is appropriately suitable for recording materials with an orthotropic fibrous structure and highlights the destruction of the reinforcement fibers, delamination of the material and interfiber destruction inside the material.

The destruction of a separate GCR fiber is described in terms of maximum values of permissible stresses or strains:

$$f_f = \frac{\sigma_1}{X} = 1 \; if \; \sigma_1 \geq 0 \text{ то } X = X_t \, , \sigma_1 < 0 \text{ то } X = X_c \tag{18}$$

$$f_m = \frac{\varepsilon_1}{X_\varepsilon} = 1 \; if \; \sigma_1 \geq 0 \text{ то} X_\varepsilon = X_{\varepsilon t} \, , \sigma_1 < 0 \text{ то } X_\varepsilon = X_{\varepsilon c} \tag{19}$$

If we consider the destruction of the matrix material, the dependence will take the following form [10]:

$$f_m = \frac{\sigma_2^2}{Y_t Y_c} + \left(\frac{\tau_{12}}{S}\right)^2 + \left(\frac{1}{Y_t} + \frac{1}{Y_c}\right)\sigma_2 \tag{20}$$

where X, Y are material strength limits for uniaxial tension or compression; R, S are material strength limits on shear.

As in many criteria, the destruction is considered to be the moment when the relative strength reaches 1. Therefore, the function takes the form [10]:

$$f_m = max(f_f, f_m) \tag{21}$$

Due to the twisting of the GCR fibers, an additional reduction coefficient should be introduced to calculate the delamination (for the rebar it is $f_w^{if} = 0{,}945$), which eventually leads to the following formula [10]:

$$\frac{1}{f_w^{if}} \sqrt{\left[\left(\frac{1}{R_\perp^+} - \frac{p_{\perp\psi}^+}{R_{\perp\psi}^A}\right)\sigma_n\right]^2 + \left(\frac{\tau_{nt}}{R_{\perp\perp}^A}\right)^2 + \left(\frac{\tau_{n1}}{R_{\perp\parallel}^A}\right)^2} + \frac{p_{\perp\psi}^+}{R_{\perp\psi}^A}\sigma_n = 1 \quad at \; \sigma_n \geq 0 \tag{22}$$

$$\text{то } \frac{1}{f_w^{if}} \sqrt{\left[\left(\frac{p_{\perp\psi}^-}{R_{\perp\psi}^A}\right)\sigma_n\right]^2 + \left(\frac{\tau_{nt}}{R_{\perp\perp}^A}\right)^2 + \left(\frac{\tau_{n1}}{R_{\perp\parallel}^A}\right)^2} + \frac{p_{\perp\psi}^-}{R_{\perp\psi}^A}\sigma_n = 1 \; at \; \sigma_n < 0 \tag{23}$$

The constants for the GCR layers have the following values:

$$p_{\perp\perp}^+ = 0{,}18; p_{\perp\perp}^- = 0{,}18; p_{\perp\parallel}^- = 0{,}24; p_{\perp\parallel}^+ = 0{,}285.$$

- Steel is an isotropic material by structure that has identical mechanical properties in all directions. However, steel reinforcement has a yield point, therefore, to specify plastic deformations, a bilinear isotropic model was adopted, according to which the yield surface expands evenly in all directions. The initial slope of the curve (σ-ε) is equivalent to the elastic modulus of the material. Beyond the limit, an increase in plastic deformation is observed. To describe this dependence, the concept of "tangent modulus", which cannot be less than zero or greater than the elastic modulus, was introduced. The maximum equivalent stresses according to Mises are used as the destruction criterion. For steel reinforcement used in our research it was 610 MPa.

3 Analysis of the results of mathematical modeling

The numerical simulation of the SSS in the contact area was carried out in the ANSYS 19.0 Workbench package based on the results of mechanical testing of reinforcement and concrete according to GOST 24452-80 and GOST 12004-81. The obtained mechanical characteristics of concrete and reinforcement are given in [12].

The adhesion of reinforcement samples with concrete B25 was determined using a pull-out test made on concrete cubes with a 100 mm edge according to GOST 31938- 2012. All

the samples hardened and gained strength in normal conditions (90 days, t = 20 ± 2 °C, w = 65%) [11]. The depth of the samples in concrete was l/d = 5 mm. The movement of the rebar relative to concrete was fixed by an indicator with an accuracy of 0.001 mm installed on the loaded end of the rebar.

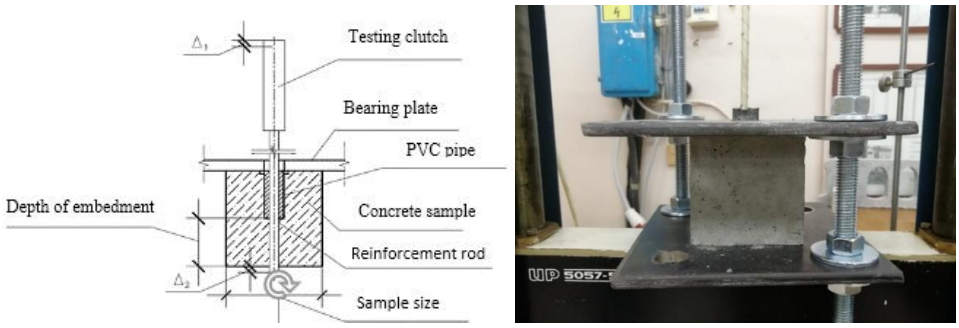

Fig. 2. The scheme of the sample for pull-out test

For convenience, the shear stress τ_{ad} was used as a result of measuring the bearing capacity:

$$\tau_{ad} = \frac{N}{lP} \tag{24}$$

where N is the force applied; l is the anchoring depth; P is a circle perimeter.

During testing, the load applied to each of the 10 samples was recorded using a force-measuring sensor. Simultaneously, the displacement of the rebar was measured (Δ) relative to the upper end of the concrete. Subsequently, a generalized curve "shear stresses - displacements" was built.

The mutual displacement of the reinforcement relative to concrete was determined by the formula:

$$\Delta = \Delta_1 - \Delta l_a \tag{25}$$

where $\boldsymbol{\Delta_1}$is the fixed value of the rebar displacement; $\boldsymbol{\Delta l_a}$ is the reinforcement elongation between fasteners and the reference end of the sample, which was defined as:

$$\Delta l_a = \frac{Nl}{AE_a} \tag{26}$$

where l is the initial length of the reinforcement between the fastener and the reference end of the sample; A is a rebar area; $E_a$is an elastic modulus of the reinforcement.

Fig. 3 shows the convergence of the experimental data with the results of numerical simulation. It can be seen that the model describes the rebar displacement in the concrete mass. However, the maximum value of the bearing capacity was 5% lower than during the experiments. This is due to the fact that a smaller amount of plastic deformations in the concrete mass was put into the model. It should also be noted that the nature of the shifts initially represented a linear relationship, which was reflected by the actual shift schedule. For a more accurate reflection of the first solution stage, we had to add two additional conditions. Firstly, at the first loading stage, there is a gluing effect of the cement gel which takes the form presented in the formula 6. Secondly, this is the reinforcement compression by the concrete mass due to shrinkage and hardening of the concrete (Fig. 4). Furthermore, these conditions are not used in the calculation of the inelastic stage of the material, which allows to obtain a more accurate match of the calculated and experimental data for the entire range of materials.

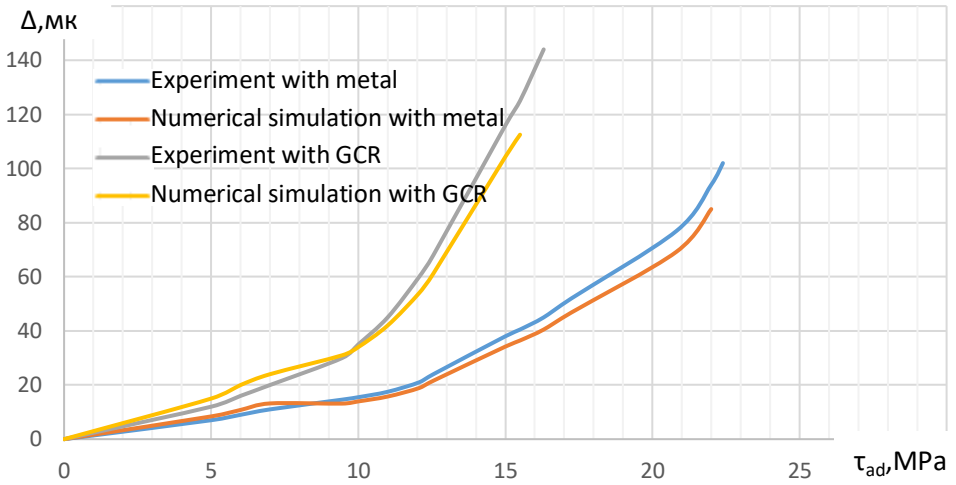

Fig. 3. Dependency "shear stresses - displacements"

4 Stress-strain state in a concrete mass

The paper deals with the SSS in a concrete mass with a force equal 0.85 of the destruction load. At higher loads, an avalanche-like increase in stresses and plastic deformations is observed, which is not interesting for us.

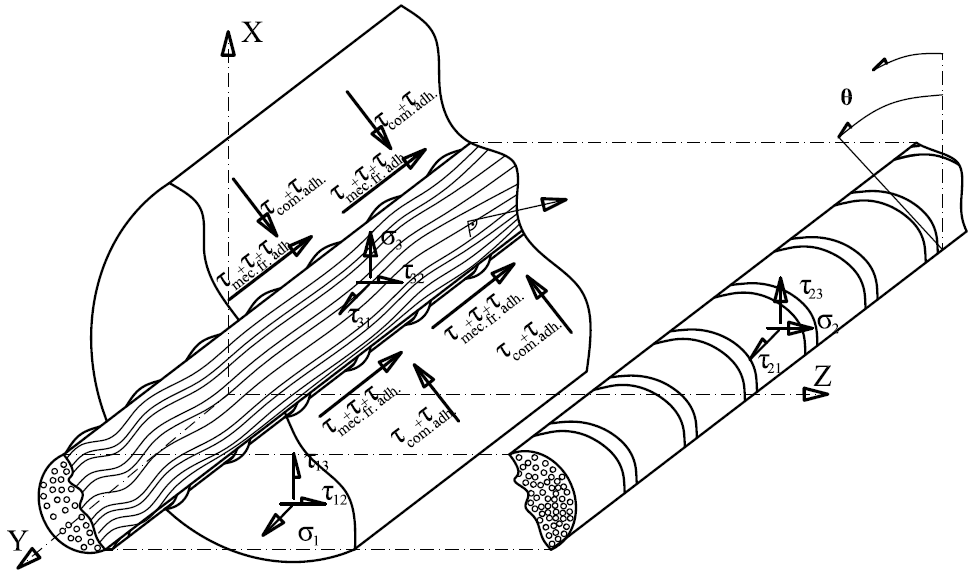

Fig. 4. Distribution of adhesion forces of reinforcement periodic profile with concrete

It should be noted that the magnitude of adhesion, and, as a result, the SSS in the embedment area consists of a number of factors shown in Fig.4. The fundamental factor is the mechanical mesh of the rebar periodic profile with the concrete consoles. When considering the SSS, it is important to pay special attention to the concrete consoles formed between reinforcement profiles. Fig. 4 shows consoles from the two sides which in parallel take the distribution of compressive stress arising from the load transfer by the

reinforcement profile [11-18]. Besides, to fulfill the equilibrium condition, tensile stresses are formed in the upper face.

For the composite reinforcement, due to the lower stiffness of the profile, the concrete consoles fully work in compression, and since the profile is threaded at an angle of 30 degrees, the compression platform is formed at the same angle between the profile windings for equilibrium (Fig. 5b). The rest of the mass works on longitudinal tensile stresses in the Y plane.

a) b)

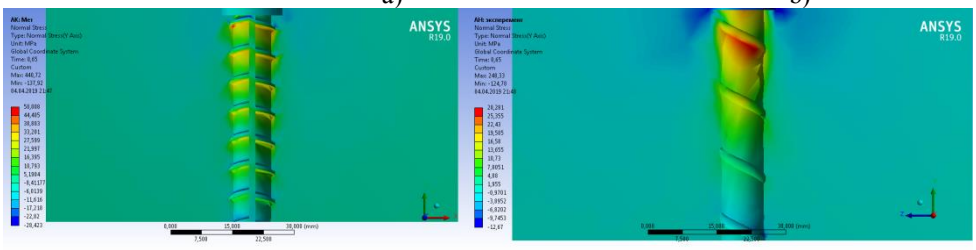

Fig. 5. Distribution of normal stresses along the Y axis of the samples in the concrete mass: a) metal reinforcement; b) GCR

a) b)

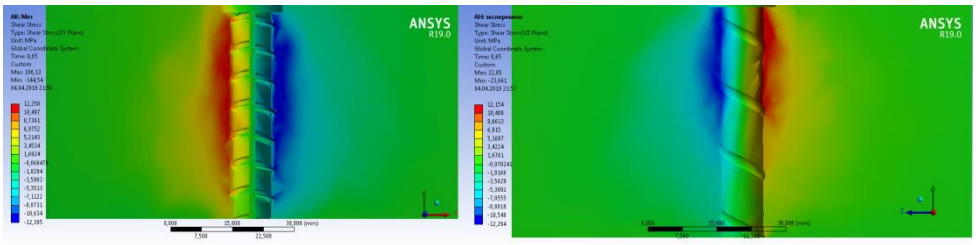

Fig. 6. Distribution of shear stresses along the XY plane of the samples in the concrete mass: **a)** metal reinforcement; **b)** GCR

Kholmyansky M.M. noted that the classic concept of engineering strength of the concrete for solving the contact problem is incorrect to use. Therefore, to solve the problem, it is required to use the strength characteristics of concrete on a scale of 1 - 0.01 mm.

It is known [1] that increasing the sample sizes leads to increasing the probability of microdefects in the material structure. Therefore, when decreasing the sample sizes, the strength of concrete usually increases. In this case, it is confirmed by the fact that the maximum compressive stresses formed under the consoles reach 100 MPa, while tensile stresses are up to 2 MPa and more.

The results for comparing mutual shear stresses along the XY plane are presented in Fig. 6. The dependence of stresses takes an exponential form for both reinforcements; however, the magnitude has different values, since there are leaps in the place of the periodic profile, which are about 4 times lower for GCR than for steel. This is due to the higher elastic modulus and the homogeneous structure of the metal reinforcement, which in turn leads to pronounced leaps. When the embedment depth increases, the shear stresses of both reinforcements smoothly fade out (Fig. 7.).

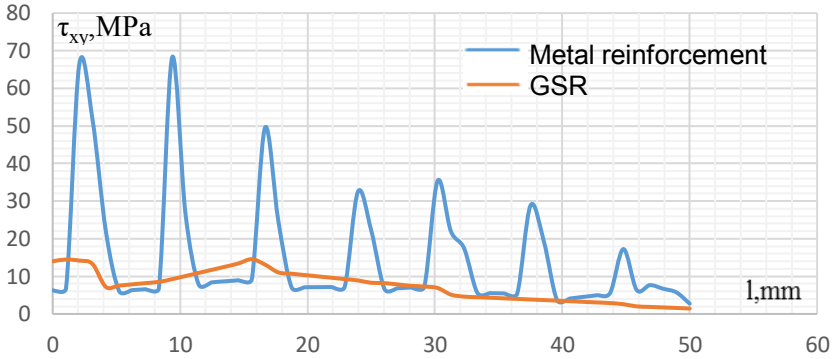

Fig. 7. Shear stress distribution on the XY plane along the embedment depth

When considering plastic deformations, it can be seen that they are formed in those places where later the formation of cracks and the subsequent destruction of the adhesion will occur. For example, for the samples with metal reinforcement plastic deformations are formed in the cut-off areas of concrete consoles (Fig. 8a), while for GCR deformations these deformations are pronounced only along the main rebar in the planes of compressive stresses (Fig. 8b).

a) b)

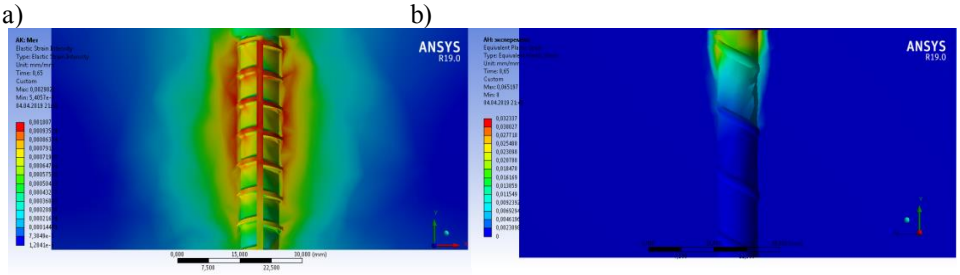

Fig. 8. Maximum plastic deformations in a concrete mass: a) metal reinforcement; b) GCR

5 Damage accumulation in reinforcement

Experimental studies with steel reinforcement showed that the destruction of the rebar did not occur. So the maximum stress from the destruction load reached 0.783. At the same time, the value from the destruction load in the rebar periodic profile in the embedment area was 0.25. This testifies to the fact that during the pull-out testing the steel reinforcement profile did not exhaust its reserve, and the decisive reason was the destruction of concrete in the contact area.

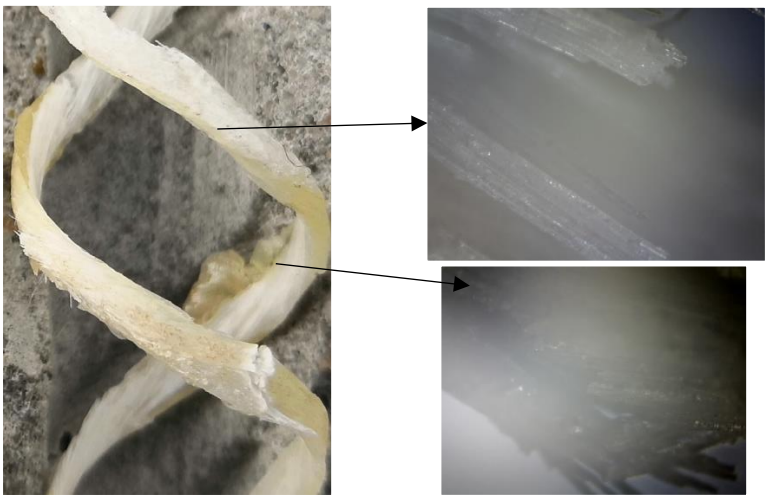

Fig. 10. Failure in the GCR periodic profile

When considering a numerical model with GCR, the adhesion failure occurred between the main rebar and the periodic profile (CZM). In addition, the reinforcement showed the damage from tensile and compressive stresses in the GCR periodic profile. Their values were 1.579 and 1.065 from the Puck destruction load (Fig. 11 b, c), which was confirmed experimentally (Fig. 10).

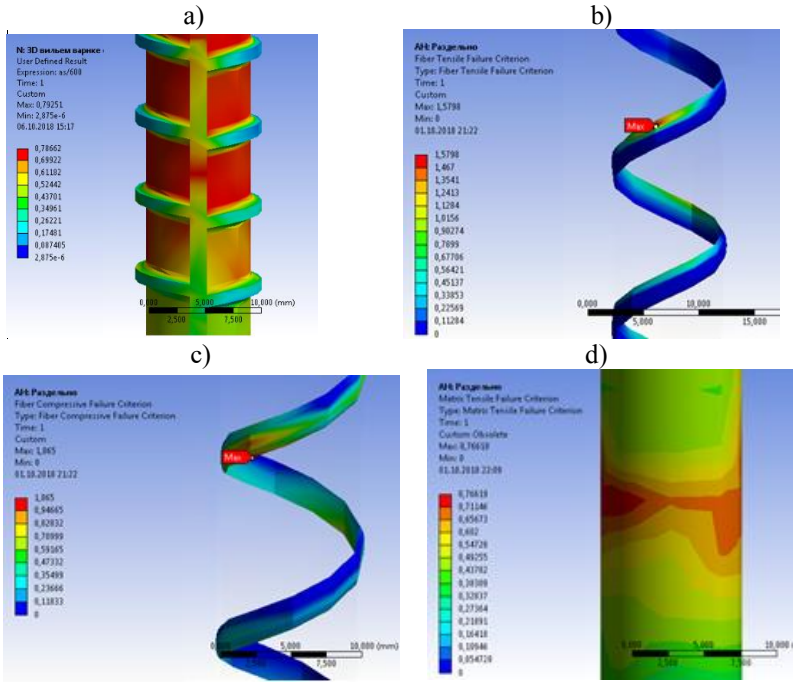

Fig.11. Damage accumulation in the reinforcement: **a)** metal; **b)** fibers under tensile stress in GCR; **c)** fibers under compressive stress in GCR; **d)** matrices under tensile stress in GCR

It should be noted that the destruction load of the matrix under the tensile stress in the embedment area of the main rebar was 0.76 by Puck. This explains the rare cases during testing, when the reinforcement was destructed along the rebar without cutting off the

periodic profile (Fig.11d). The same destruction was observed when testing the GCR with the embedment depth of $l/d \geq 6$, since the destruction value of the matrix increased to 0.97 by Puck, and the strain intensity value was below the maximum by 15%.

Conclusion

1. The analysis of existing models of concrete deformation showed that the Menetrey-Willam model should be used to consider the distribution of stresses in the contact layer of concrete, taking into account hardening and softening of the concrete mass.
2. The developed numerical model of reinforcement adhesion with concrete has expanded the existing ideas about the SSS in the contact area of concrete with reinforcement. This allowed to establish the nonlinear character of the distribution of shear and normal stresses over the entire embedment depth. Thus, leaps of stresses are observed in the contact area of concrete and reinforcement periodic profile, which become the cause of major cracks.
3. The numerical simulation of the GCR embedment in the concrete mass based on the ANSYS 19.0 Workbench software package according to the previously determined mechanical characteristics of materials allowed to determine the nature of the damage accumulation in the reinforcement and to reveal that the destruction of composite reinforcement occurs from tensile stresses by breaking the fibers or the GSR matrix.

References

1. A. V. Benin, A. S. Semenov, S. G. Semenov, Adv. Civ. Eng. Buld. M 233 (2013) DOI: 10.5862/MCE.40.10
2. G. L. Balazs, B&S **102**, 46 (2007)
3. W. C. Schnobrich, M. Suidan, ASCE ST10 **10**, 2109 (1973)
4. V. I. Travush, D. V. Konin, L. S. Rozhkova, A. S. Krylov, D F E R S E C, **5**, 31 (2016)
5. ANSYS *Mechanical APDL theory reference* **15.0.** (Canonsburg, Pennsylvania, USA, 2013)
6. P. Menetrey, *Numerical Analysis of Punching Failure in Reinforced Concrete Structures* (1994)
7. K. J. Willam, E. P. Warnke, IABS, **19**, 1 (1975)
8. D. C. Drucker, W. Prager, QAM, **10**, 157 (1952)
9. G. G. Kashevarova, A. S. Martirosyan, V.I. Travush, VPNIPM, **3**, 62 **(**2016)
10. A. Puck, L. Amleh, A. Ghosh, Can J Civ Eng. **33**, 673 (2006)
11. A. N. Nikolyukin, V.P. Yartsev, I.I. Kolomnikova, D.Z. Aljaboobi, TCM, **1** (2019) DOI: 10.15862/02SATS119
12. Z. P. Bazant, B. H. Oh, JEM **111**, 559 (1985)
13. Jirasek, *Numerical Modeling of Deformation and Failure of Materials* (Lecture notes. 2000)
14. W. F. Chen, Plast. Modl. 2 (1994)
15. A. S. Martirosyan, V. I. Travush, G. G. Kashevarova, PNRPU **1**, 147 (2017) DOI: 10.15593/2409-5125/2017.01.13
16. P. Launay, H. Gachon, Special publication, **34**, 269 (1972)
17. Y.D. Murray, *User's manual for LS-DYNA concrete material model 159* (2007)
18. K. Lundgren, K. Gylltoft, Mag. of CR **52**, 53 (2000)